Neuroscience 161 (2009) 655–662

VISUAL ADAPTATION TO CONVEXITY IN MACAQUE AREA V4

K.-M. MÜLLER,[a,b] M. WILKE[a,c] AND D. A. LEOPOLD[a,d,e]*

[a]*Unit on Cognitive Neurophysiology and Imaging, Laboratory of Neuropsychology, National Institute of Mental Health, National Institutes of Health, Building 49, Room B2J–45 MSC 4400, 49 Convent Drive, Bethesda, MD 20892, USA*

[b]*International Max Planck Research School, University of Tübingen, Germany*

[c]*Division of Biology, California Institute of Technology, Pasadena, CA, USA*

[d]*National Institute for Neurological Disorders and Stroke, NIH, USA*

[e]*National Eye Institute, NIH, USA*

Abstract—Aftereffects are perceptual illusions caused by visual adaptation to one or more stimulus attribute, such as orientation, motion, or shape. Neurophysiological studies seeking to understand the basis of visual adaptation have observed firing rate reduction and changes in tuning of stimulus-selective neurons following periods of prolonged visual stimulation. In the domain of shape, recent psychophysical work has shown that adaptation to a convex pattern induces a subsequently seen rectangle to appear slightly concave. In the present study, we investigate the possible contribution of V4 neurons of rhesus monkeys, which are thought to be involved in the coding of convexity, to shape-specific adaptation. Visually responsive neurons were monitored during the brief presentation of simple shapes varying in their convexity level. Each test presentation was preceded by either a blank period or several seconds of adaptation to a convex or concave stimulus, presented in two different sizes. Adaptation consistently shifted the tuning of neurons away from the convex or concave adapter, including shifting response to the neutral rectangle in the direction of the opposite convexity. This repulsive shift resembled the known perceptual distortion associated with adaptation to such stimuli. In addition, adaptation caused a nonspecific response decrease, as well as a specific decrease for repeated stimuli. The latter effects were observed whether or not the adapting and test stimuli matched closely in their size. Taken together, these results provide evidence for shape-specific adaptation of neurons in area V4, which may contribute to the perception of the convexity aftereffect.

Key words: visual perception, visual cortex, area V4, electrophysiology, adaptation, visual aftereffects.

A visual stimulus presented on two separate occasions will inevitably elicit different responses from the brain (Faisal et al., 2008). Response variability of single neurons is contributed in part by endogenous factors such as ongoing activity (Arieli et al., 1995) and cognitive variables such as attention (Desimone and Duncan, 1995). At the same time, exogenous factors such as stimulation history can significantly influence the response elicited by a given presentation. For example, the prolonged or repeated exposure to a visual stimulus, often termed adaptation, can significantly alter the response of neurons at all stages of visual processing. Repeated stimulation of the same portion of the retina leads to declining responses from ganglion cells (Enroth-Cugell and Shapley, 1973; Brown and Masland, 2001) as well as neurons throughout the visual brain (Maffei et al., 1973; Miller et al., 1991; Lisberger and Movshon, 1999). At the behavioral level, visual adaptation can alter the subsequent perception of visual stimuli in many visual domains such as orientation (Gibson, 1937; Gibson and Radner, 1937), motion (Anstis et al., 1998; Addams, 1834), spatial configuration (Köhler and Wallach, 1944), color (Webster and Mollon, 1991), or complex shape (Webster and MacLin, 1999). Perceptual aftereffects thereby serve as an important avenue for visual scientists to understand neural principles of stimulus encoding (Frisby, 1979).

Recent work has highlighted the usefulness of adaptation for studying shape perception (Gheorghiu and Kingdom, 2008; Webster and MacLin, 1999; Leopold et al., 2001). In a series of studies, Suzuki (2001, 2003), demonstrated that aftereffects for shape could be observed following adaptation to intermediate-level stimulus features such as convexity and concavity. Specifically, brief exposure to convex shapes was shown to cause subsequently presented rectilinear shapes to appear concave and vice versa; an attention-dependent effect the author took as evidence for opponency in the domain of shape. In considering its neural basis, Suzuki initially postulated that neurons in the inferotemporal cortex could underlie the shape specific aftereffect, based largely on the fact that aftereffect could be observed despite a mismatch in the relative scales of the adapting and test stimuli (Suzuki, 2001; Suzuki and Cavanagh, 1998). Based on further experiments (Suzuki, 2003), along evidence from the neurophysiology of attention (Reynolds et al., 1999), area V4 was identified as a more likely candidate. This speculation resonates with other studies that have identified area V4 as being instrumental in the intermediate level processing of shape, including both lesion studies (Merigan and Pham, 1998; Merigan, 2000) and microelectrode recordings (Kobatake and Tanaka, 1994; Pasupathy and Connor, 2001, 2002; Hegde and Van Essen, 2007). In a pivotal study Pasupathy and Connor (1999) concluded that V4 neurons express a systematic tuning to contour features and, based on tuning to a large number of parametrically

*Correspondence to: D. A. Leopold, Unit on Cognitive Neurophysiology and Imaging, Laboratory of Neuropsychology, National Institute of Mental Health, National Institutes of Health, Building 49, Room B2J–45 MSC 4400, 49 Convent Drive, Bethesda, MD 20892, USA. Tel: +1-301-594 0582.
E-mail address: leopoldd@mail.nih.gov (D. A. Leopold).

0306-4522/09 $ - see front matter
doi:10.1016/j.neuroscience.2009.03.070

manipulated colored shapes, singled out convexity as a key determinant of V4 cell responses.

The present study directly examines the effects of adaptation upon the responses to convex and concave stimuli in area V4. We focus on the relationship of neural adaptation effects to the previously reported perceptual aftereffect as well as the robustness of adaptation effects to the size of the adapting stimuli.

EXPERIMENTAL PROCEDURES

Surgery and animal handling

All described procedures were carried out under a protocol approved by the Animal Care and Use Committee of the National Institute of Mental Health. They are in accordance with the National Institutes of Health Guide for the Care and Use of Laboratory Animals. Great care was taken to minimize the number of animals used in the study, and to avoid any pain or discomfort during experimental testing.

Two male adult rhesus macaques (*Macaca mulatta*, "monkey B" (7.8 kg) and "monkey E" (8.0 kg)) underwent surgery under sterile conditions and deep isoflurane anesthesia. Custom head restraints constructed from G10 fiberglass were implanted using transcranial ceramic screws (Thomas Recording, Giessen, Germany) and self-curing dental acrylic (Lang Inc., Wheeling, IL, USA). Scleral search coils were implanted (Judge et al., 1980). Then, the animals were trained to maintain their gaze within a window of 0.5° radius using apple juice as positive reinforcement. In a later surgery, each monkey was implanted with a custom-made recording chamber targeting ventral V4, which was installed using magnetic resonance imaging (MRI) guided surgery software (BrainSight primate, Rogue Research, Montreal, QC, Canada), and craniotomy was performed. Recording sites were determined by MRI anatomical criteria (Saleem and Logothetis, 2007; Paxinos et al., 2000). In order to acquire anatomical images, a 4.7 T, 60 cm vertical monkey scanner (Bruker Biospec) equipped with a Siemens AC44 gradient coil was used. Using positive reinforcement, monkeys were trained to accept the scanner environment and sat in a custom-made MR-compatible chair without the necessity for anesthesia. The animals were scanned using custom-made radiofrequency coils. Coronal anatomical images were acquired using a modified driven equilibrium Fourier transform (MDEFT) sequence with slice thicknesses of 0.7 or 1 mm, allowing us to immediately verify recording positions following the physiological recording (Matsui et al., 2007).

Equipment and data acquisition

Stimuli were created on a PC workstation and in the case of monkey B displayed on a 33.5×59.5 cm/1024×768 pixel screen with a viewing distance of 100 cm. For monkey E a 38×65 cm/1024×768 pixel screen was used with a viewing distance of 88 cm. Custom written software was used for stimulus presentation (Stim, QPCS, courtesy David Sheinberg).

Single units were monitored in ventral cortical area V4 with standard extracellular recording techniques, using commercially available 20 μm diameter tungsten electrodes coated with glass (outer diameter: 80 μm; impedance: 0.7–2.0 MΩ at 1 kHz; Thomas Recording). At the beginning of each recording session, an Eckhorn multielectrode array (Thomas Recording) was used to lower two to seven microelectrodes simultaneously into the brain through a 25 gauge guide tube. The microelectrodes were advanced individually and positioned within area V4. A metallic plate located in the saline-filled chamber was used as both reference and ground. The raw signal was preamplified within the Eckhorn array and subsequently amplified, high-pass filtered, and digitized (Plexon Inc., Dallas, TX, USA). Spike candidates were identified online through Rasputin software (Plexon Inc.) on a PC receiving the digitized signals. We adjusted the waveform thresholds manually for each channel immediately before the recording file was started. After the experiment, units were isolated in principal component analysis (PCA) space in the commercially available "Off-

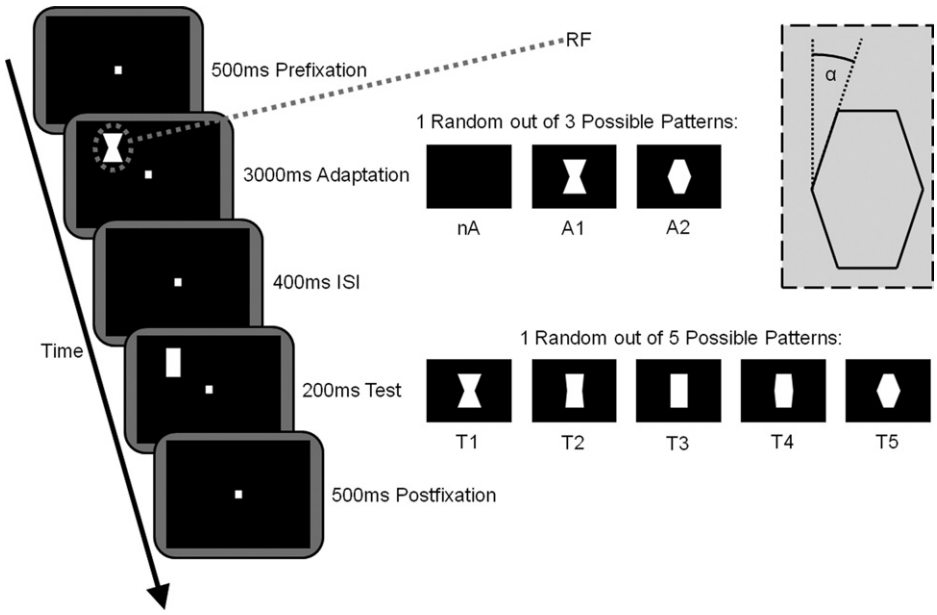

Fig. 1. Visual stimulation paradigm. Monkeys held their gaze on a fixation dot while stimuli were presented completely within a previously mapped receptive field. On adaptation trials, 3 s exposure to A1 or A2 was followed by the presentation of the test pattern. Baseline tuning was determined in the absence of any adaptation pattern (nA). Completion of successful trials was rewarded with apple juice. The inset illustrates angle α; see "Experimental Procedures" section for details (nA, A1, A2=adaptation stimuli; T1–T5=test stimuli; RF=schematic of manually mapped receptive field; ISI=interstimulus interval).

line Sorter" (Plexon Inc.), and timestamps were saved for further processing.

Receptive field mapping

Once a neuron was identified on an oscilloscope, the extent of its receptive field (minimal response field) was determined using custom written software. The monkey fixated on a square subtending as little as 3 min of visual angle, while white bars on a black background were manually swept across the screen to identify the respective area evoking neural responses. During the sessions with more than one intact electrode, the mapping procedure was applied to all channels. Since all electrodes in a given session were separated by less than 1 mm, the receptive fields were largely overlapping. Supplementary Fig. 3 yields detailed information about the receptive field properties.

Task and stimuli

Based on the receptive field plotting, the stimuli were adjusted to be smaller than the receptive fields, and fit completely into the measured boundaries (see Supplementary Fig. 3C). The visual paradigm is depicted in Fig. 1. Once the monkey acquired fixation, the sequence of visual stimuli started: Following a 500 ms baseline period, an adaptation pattern was shown for 3000 ms. Then, after a 400 ms blank interval, the test stimulus was shown for 200 ms. A 500 ms poststimulation fixation period followed. The adaptation phase was characterized by either no visual stimulation (nA) or else concave or convex adapters of the same size as the test stimuli (A1 or A2). In all sessions, larger adapters of the same shape with an area 2.25 times the standard stimulus size were presented as well (not shown in Fig. 1). All stimuli were solid white (luminance 41 cd/m^2) on a black background (luminance 0.1 cd/m^2) and were always presented in the upright orientations as shown in Fig. 2. We define the level of convexity through angle α as illustrated in Fig. 1. For adapters, two levels of convexity were used: $\alpha=-21.8°$ (concave, A1) and $\alpha=21.8°$ (convex, A2). The test stimuli consisted of five different convexity levels: $\alpha=-21.8°$ (T1), $\alpha=-5.7°$ (minimally concave, T2), $\alpha=0°$ (rectangular, aspect ratio ½ (width/height), T3), $\alpha=5.7°$ (minimally convex, T4), and $\alpha=21.8°$ (T5). All test stimuli and standard size adapters (A1 and A2) were of the same area. The change in convexity was achieved by varying the width of the stimuli, while keeping the height constant. Overall this stimulus arrangement resulted in 25 different combinations of adaptation and test stimuli. These 25 combinations were presented in random order. A session lasted 500 trials, providing 20 trials per condition on average.

The animal was required to maintain fixation over the length of a trial (4600 ms) in a 0.7° radius window (occasionally this was changed to other values between 0.5° and 0.8°, e.g. due to training or motivational purposes). Successful fixation was rewarded with a drop of apple juice. Breaking fixation would abort the trial immediately and prevent the animal from being rewarded. Aborted trials were excluded from further analysis. Between trials there was a 2000 ms break.

Analysis

Analysis was performed using custom written code in MATLAB 7.4 (Mathworks Inc., Natick, MA, USA). Neural responses were analyzed in a window from 80 ms after test stimulus onset until 80 ms after test stimulus offset (i.e. 80–280 ms post–test stimulus onset). This time range ensured the inclusion of the full visual response to the test stimulus while excluding potential "offset responses" as observed in several neurons. We also tested other plausible analysis windows, but the results did not change.

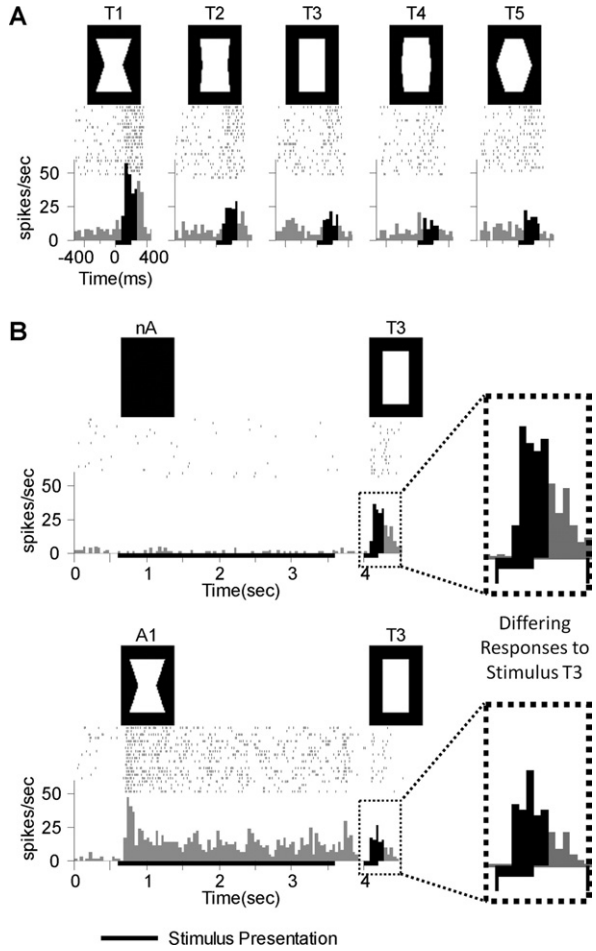

Fig. 2. Typical V4 responses to stimulus set. Spike rasters are shown above with peristimulus time histograms below. Black vertical histogram bars designate the analysis window (80–280 ms post–test onset). (A) Selective response of a unit in the absence of adaptation (cf. Fig. 1: nA). (B) A different unit. In this example as well as on the average population level adaptation reduced the response. The entire response profiles over all five adaptation conditions including all full trial responses for the two units in this figure are presented in Supplementary Figs. 1 and 2, respectively.

RESULTS

We recorded from 154 single units in ventral area V4 of two monkeys, out of which 104 were visually responsive, in the context of an adaptation paradigm similar to that used to demonstrate the attention-dependent psychophysical aftereffect for convexity (Suzuki, 2001, 2003). The monkeys did not report their percept, but were required to maintain fixation steadily through the adaptation and test periods. We began by evaluating the convexity tuning of each neuron in the absence of any adaptation. In this baseline condition 38 (37%) of the neurons responded selectively as a function of convexity level (univariate ANOVA, $P<0.05$). An example of such a neuron, tuned for the most concave stimulus (T1), is shown in Fig. 2A. Of the selective neurons, 68% (26 out of 38) responded strongest to the most concave stimulus, 8% (three out of 38) to the most convex stimulus, and 24% (nine out of 38) to

the neutral stimulus or one of the minimal deviations thereof.

We next asked how the pattern of responses to the test stimuli might be influenced by a period of prior shape adaptation, focusing first on responses to the neutral (i.e. rectangular) test stimulus. Adaptation significantly affected the responses of 44% of the neurons tested (univariate ANOVA over three adaptation condition mean values, $P<0.05$), leading to an average absolute shift in firing rate of 5.9 spikes/s (mean over all unadapted compared to mean over all adapted). Across the population, this adaptation was shape-specific, inducing a change in firing rate consistent with the expectations of a negative perceptual aftereffect. We assessed this by comparing the responses to the neutral test stimulus following adaptation to those elicited by low convexity levels in the absence of adaptation. Since adaptation caused an overall decrease in firing, we calculated response *differences* for the adapted condition (neutral test) and the unadapted condition (lower convexity tests). Specifically, we asked whether a shift in the response to a neutral stimulus following convex or concave adaptation (effect of adaptation) would be predicted by the neuron's tuning to low-convexity levels (effect of convexity level). There is some reason to expect a negative correlation, since an aftereffect following adaptation to convexity results in the percept of concavity, and vice versa. Indeed, we found that for units with a preference for a convex stimulus, responses to the neutral stimulus were more strongly suppressed following adaptation to the convex than to the concave stimulus, and vice versa. The effect of adaptation on the response is plotted against the effect of tuning in Fig. 3, revealing a significant negative correlation between these measures. Note, when there was a *mismatch* in the size of the adapting and test stimuli, this negative correlation disappeared across the population (cf. Supplementary Fig. 4; 38 U, $r=0.15$, $P=0.38$, NS), though it was present in some neurons (e.g. Supplementary Fig. 2).

Next, we analyzed neural responses to five different convexity levels following three seconds of exposure to convex or concave adapters (see Fig. 2B). The relative responses were computed for each unit prior to averaging by subtracting the mean baseline response to the five test stimuli. The mean results across the population ($n=104$) are shown in Fig. 4A. In the absence of adaptation, the

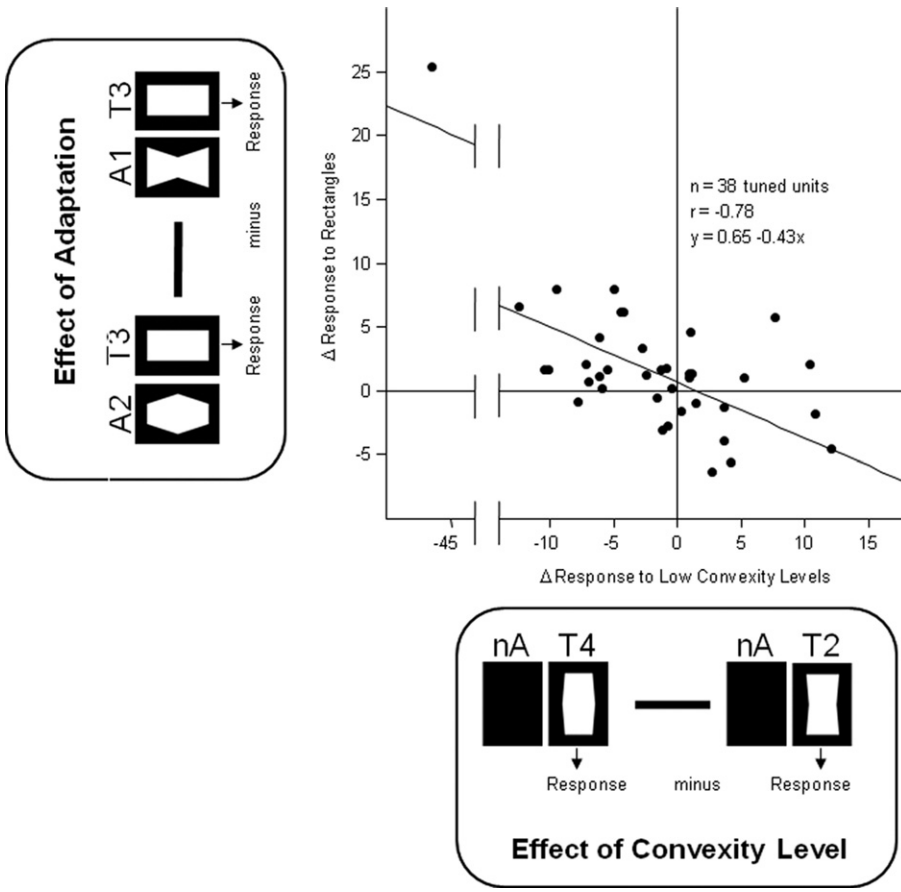

Fig. 3. Negative correlation between convexity tuning and the effects of adaptation on the response to the zero-convexity test stimulus. All single units with significant tuning to one of the five test stimuli were included in this analysis, with each dot corresponding to one unit. Values on the x-axis show responses to low convexity levels without previous adaptation (nA): mean firing rate to T2 was subtracted from mean firing rate to T4. The y-axis shows differential effects of convex (A2) and concave (A1) adaptation on response to a test rectangle (T3). Note the high correlation with negative slope between the two differential measures, indicative of a negative aftereffect (38 units, $r=-0.78$, $P<0.01$). The correlation did not depend on the strongest data point as shown in Supplementary Fig. 5 (excluding one outlier: 37 units, $r=-0.46$, $P<0.01$).

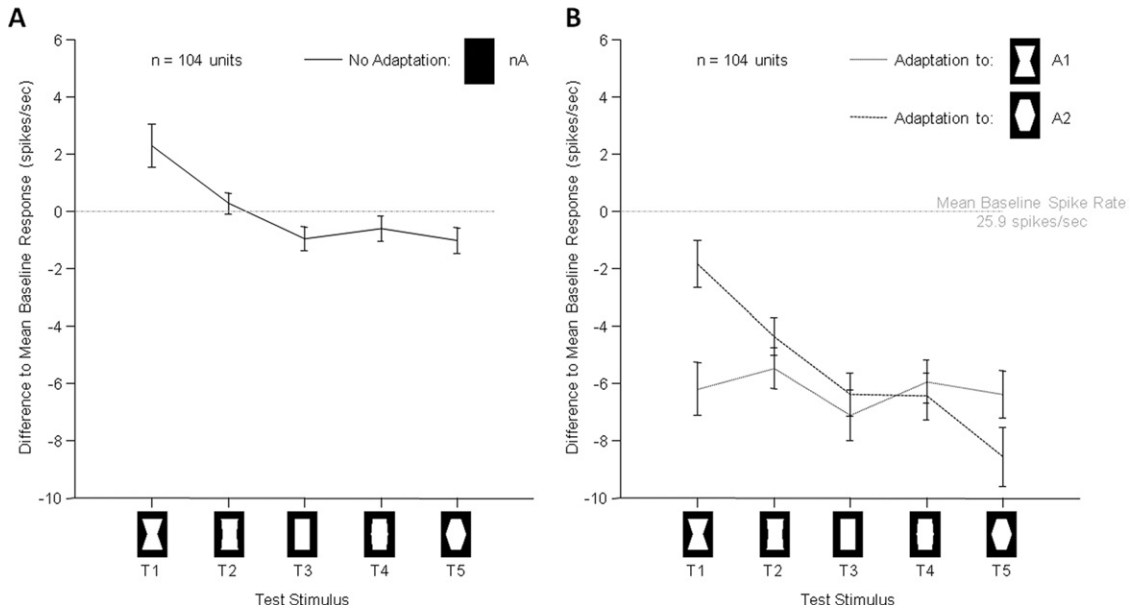

Fig. 4. Nonspecific and specific effects of adaptation. The y-axis marks the difference to the mean baseline activity. X-axis shows the different test stimuli. Error bars represent the standard error of the mean. (A) Average response to the test stimuli across the population. Note the overall preference to the globally concave stimulus. (B) Population tuning following adaptation. Note that the most prominent effect was a significant overall decrease in firing following adaptation. In addition there was a smaller stimulus specific effect of adaptation, which can be inferred by comparing the responses to T1 and T5 following different adapters.

most concave stimulus gave a slightly but significantly higher response compared to the other stimuli. While this result apparently contradicts previous findings in dorsal V4 (Pasupathy and Connor, 1999), and TE (Kayaert et al., 2005), where convex patterns were shown to be preferred over concave ones across the population, there may be simple explanations for this finding. Namely, the concave patterns contain more contrast in the center of the receptive field as well as more acute angles on their boundaries compared to the convex stimuli. It may then be that V4 neurons respond more strongly to acute boundary fragments, which is consistent with the findings in previous studies.

Fig. 4B shows that adaptation led to a large, nonspecific decrease in responses for all test stimuli across the population (assessed through two separate two-way ANOVAs, “no adaptation” vs. “convex adapter”: main effect

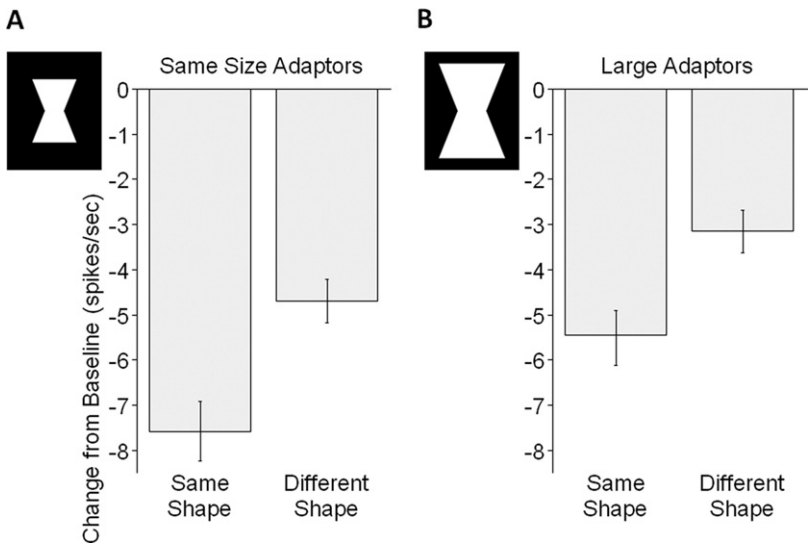

Fig. 5. Size-independent pattern specificity of adaptation ($n=104$ single units, two conditions per unit combined in each data point). Here, the pooled effects of the convex and the concave adapters onto T1 or T5 respectively are depicted. The stimuli illustrate the size difference. Convex adapters were of the same area as the concave adapters shown here. (A) Average difference between adapted and baseline firing is 7.6 spikes/second for the same shapes vs. 4.7 spikes/second for different shapes. Error bars indicate standard error of the mean. (B) Larger size refers to adapters of the same shapes but 2.25 times the area. Note that the pattern selective adaptation effect remains despite a change in the adapter size.

$F(1,1039)=186.1$, $P<0.001$; "no adaptation" vs. "concave adapter": main effect $F(1,1039)=262.0$, $P<0.001$). Note that this result relates to mean overall activity, rather than a characteristic single unit example. Next to this nonspecific decrease over the population, the effects evoked by adaptation and test stimuli interacted. A two-way ANOVA, comparing the different conditions in Fig. 4B revealed a significant interaction ("adapter convexity" vs. "test convexity": interaction $F(4,1039)=262.0$, $P<0.001$).

Further analysis showed that the significant interaction in Fig. 4B was caused by the special case when adapting and test stimuli were of the same shape. Fig. 5 shows that, for equal patterns, there was stronger decrease in subsequent neural activity as compared to differently shaped adapters. This effect is reminiscent of pattern specific repetition suppression observed in more rostral temporal areas (Miller et al., 1991; Sobotka and Ringo, 1994; Brown and Xiang, 1998) but also well documented for the early visual cortex (Carandini et al., 1997). The mean effects of adaptation for individual neurons across the population can be seen in Fig. 5A, which shows that the strongest suppression follows adaptation to the same convexity. Note that this effect was also observed if the adapting stimuli were 2.25 times larger in area (Fig. 5B), suggesting that the repetition-suppression effect, unlike the adaptation to neutral stimulus (Fig. 3) has some degree of tolerance for scale.

DISCUSSION

Neural responses in area V4 were strongly influenced by prior adaptation, and this influence consisted of three components. The first, *nonspecific*, component resulted in a suppression of neural firing rate across the population regardless of the identity of the test and adapting stimuli (see Fig. 4). The second, *shape-specific*, component resembled the well-studied phenomenon of repetition suppression. This effect is characterized by prior exposure to the same stimulus inducing a stronger suppression than prior exposure to a different stimulus (see Fig. 5). Repetition suppression contingent upon specific stimuli has been reported in different visual areas of the ventral stream preceding and following V4 (Miller et al., 1991; Carandini et al., 1997; Sawamura et al., 2006). The third and most complex component of adaptation was both *shape-* and *tuning-specific* (Fig. 3). In this component, which can be compared directly to the corresponding shape aftereffect, the neural response to a neutral stimulus was shifted away from the adapting stimulus according to each neuron's tuning function.

Adaptation in the early visual system is well documented, and may account for the nonspecific component in the present study. In the precortical cascade of events from photoreceptors through ganglion cells and thalamic relay neurons, adaptation effects have been demonstrated (Perlman and Normann, 1998; Smirnakis et al., 1997; Sanchez-Vives et al., 2000) and have been characterized by decline of the spike rate and post-adaptation firing reduction for several seconds. One common difficulty in drawing conclusions based on the neural effects of visual adaptation is that adaptation simultaneously influences neurons at many stages of visual processing, and potentially in different ways. While at any point in the visual pathway, *some* aspects of adaptation will be inherited from previous processing stages, others may be generated locally. For contrast adaptation much of adaptation is clearly of early cortical origin (Maffei et al., 1973; Ohzawa et al., 1985; Sanchez-Vives et al., 2000). This component of V1 adaptation correlates with a tonic hyperpolarization of the cell membranes, which is likely to be the cause for the decline in spike rate and postadaptation firing reduction (Carandini and Ferster, 1997; Sanchez-Vives et al., 2000). Similarly, evidence suggests that the adaptation measured in neurons of the middle temporal area of the parietal lobe in the macaque (area MT) also has its origins in the striate cortex (Kohn and Movshon, 2003). It would therefore be expected that a large fraction of the nonspecific adaptation effects, which were on average suppressive, have their origins in primary visual cortex or earlier.

The shape- and tuning-specific component provides the first link between neural activity in V4 and a perceptual aftereffect. The parameters of the minimally convex and minimally concave stimuli were chosen to resemble the visual aftereffect (Suzuki, 2001). Previous studies examining parametric tuning characteristics of V4 neurons have concluded that shape (Pasupathy and Connor, 2001, 2002; Gallant et al., 1996; Hegde and Van Essen, 2007) and particularly convexity (Pasupathy and Connor, 1999), are important coding features of V4. The present findings suggest that this shape feature can be specifically adapted in V4 neurons, and that this adaptation results in a predictable change in the tuning of the neuron. The three components of adaptation in our results have been reported in other adaptation studies in cat V1 (Dragoi et al., 2000, 2001; Ghisovan et al., 2008), macaque V1 (Carandini et al., 1997; Dragoi et al., 2002) as well as macaque MT (Kohn and Movshon, 2004; Krekelberg et al., 2006). In V1 the tuning shifts away from the adapting stimulus, while in MT, there is an attractive shift towards the adapter. The negative correlation we observed in V4 between the tuning to low convexity levels and the rectangle following adaptation to high convexity levels is more similar to the repulsive shift in V1 than the attractive shift in MT. However, note that tuning in V4 is not as well understood as in V1 or MT, thus analyzing data in the traditional way turned out to be impossible for the current data set.

As can be seen in Supplementary Figs. 1 and 2, the neurons' reaction to adapters of different sizes was mainly determined by the shape rather than the size of the pattern. It is therefore no surprise, that some of the adaptation effects we report, namely the nonspecific firing rate decrease and the repetition suppression, were tolerant to substantial size changes between the adapting and test stimuli, and therefore not dependent on strict retinotopy. These effects could be the product of something as simple as cellular fatigue, since the spiking rate response of the cell during adaptation was a good predictor of the response to a given test stimulus. However, the third component, namely the negative shift in tuning associated with

the adaptational aftereffect, was more retinotopically specific, and did not occur when the adapter and test stimuli were of different sizes. Thus while the adapter firing rate alone predicted some aspects of adaptation, it failed to predict others. For any aftereffect, including convexity (Suzuki, 2001), an optimized retinotopic match between adapter and test results in the largest effect, and a mismatch in size or location leads to a weaker aftereffect. Our results that the correlation breaks down with incongruent adapter and test sizes, might constitute a correlate of this weakening. In summary, our results, taken together, suggest that not only are V4 neurons involved in analyzing the convexity of a shape, but that shifts in their responses may contribute to the corresponding adaptation aftereffect.

Acknowledgments—We thank our collaborators: N. Phipps and K. Smith for assistance with animal training and experimentation; C. Zhu and Dr. F. Ye for help with MRI scans; Dr. D. Sheinberg for providing some of the stimulation software; Dr. A. Maier and Dr. D. McMahon for insightful suggestions concerning data acquisition, analysis, and previous versions of this manuscript. This work was supported by the Intramural Research Programs of NIMH, NINDS and NEI at the National Institutes of Health.

REFERENCES

Addams R (1834) An account of a peculiar optical phenomenon seen after having looked at a moving body. London Edinburgh Philos Magazine J Sci 5:373–374.

Anstis S, Verstraten FAJ, Mather G (1998) The motion aftereffect. Trends Cogn Sci 2:111–117.

Arieli A, Shoham D, Hildesheim R, Grinvald A (1995) Coherent spatiotemporal patterns of ongoing activity revealed by real-time optical imaging coupled with single-unit recording in the cat visual cortex. J Neurophysiol 73:2072–2093.

Brown MW, Xiang JZ (1998) Recognition memory: neuronal substrates of the judgement of prior occurrence. Prog Neurobiol 55: 149–189.

Brown SP, Masland RH (2001) Spatial scale and cellular substrate of contrast adaptation by retinal ganglion cells. Nat Neurosci 4: 44–51.

Carandini M, Barlow HB, O'Keefe LP, Poirson AB, Movshon JA (1997) Adaptation to contingencies in macaque primary visual cortex. Philos Trans R Soc Lond B Biol Sci 352:1149–1154.

Carandini M, Ferster D (1997) A tonic hyperpolarization underlying contrast adaptation in cat visual cortex. Science 276:949–952.

Desimone R, Duncan J (1995) Neural mechanisms of selective visual attention. Annu Rev Neurosci 18:193–222.

Dragoi V, Rivadulla C, Sur M (2001) Foci of orientation plasticity in visual cortex. Nature 411:80–86.

Dragoi V, Sharma J, Miller EK, Sur M (2002) Dynamics of neuronal sensitivity in visual cortex and local feature discrimination. Nat Neurosci 5:883–891.

Dragoi V, Sharma J, Sur M (2000) Adaptation-induced plasticity of orientation tuning in adult visual cortex. Neuron 28:287–298.

Enroth-Cugell C, Shapley RM (1973) Adaptation and dynamics of cat retinal ganglion cells. J Physiol 233:271–309.

Faisal AA, Selen LP, Wolpert DM (2008) Noise in the nervous system. Nat Rev Neurosci 9:292–303.

Frisby JP (1979) Seeing: illusion, brain and mind. Oxford, UK: Oxford University Press.

Gallant JL, Connor CE, Rakshit S, Lewis JW, Van E (1996) Neural responses to polar, hyperbolic, and cartesian gratings in area V4 of the macaque monkey. J Neurophysiol 76:2718–2739.

Gheorghiu E, Kingdom FA (2008) Spatial properties of curvature-encoding mechanisms revealed through the shape-frequency and shape-amplitude after-effects. Vis Res 48:1107–1124.

Ghisovan N, Nemri A, Shumikhina S, Molotchnikoff S (2008) Synchrony between orientation-selective neurons is modulated during adaptation-induced plasticity in cat visual cortex. BMC Neurosci 9:60.

Gibson JJ (1937) Adaptation, after-effect, and contrast in the perception of tilted lines. II. Simultaneous contrast and the areal restriction of the after-effect. J Exp Psychol 20:553–569.

Gibson JJ, Radner M (1937) Adaptation, after-effect, and contrast in the perception of tilted lines. J Exp Psychol 20:453–467.

Hegde J, Van Essen DC (2007) A comparative study of shape representation in macaque visual areas v2 and v4. Cereb Cortex 17: 1100–1116.

Judge SJ, Richmond BJ, Chu FC (1980) Implantation of magnetic search coils for measurement of eye position: an improved method. Vis Res 20:535–538.

Kayaert G, Biederman I, Op de Beeck HP, Vogels R (2005) Tuning for shape dimensions in macaque inferior temporal cortex. Eur J Neurosci 22:212–224.

Kobatake E, Tanaka K (1994) Neuronal selectivities to complex object features in the ventral visual pathway of the macaque cerebral cortex. J Neurophysiol 71:856–867.

Köhler W, Wallach H (1944) Figural after-effects: an investigation of visual processes. Proc Am Philos Soc 88:269–357.

Kohn A, Movshon JA (2003) Neuronal adaptation to visual motion in area MT of the macaque. Neuron 39:681–691.

Kohn A, Movshon JA (2004) Adaptation changes the direction tuning of macaque MT neurons. Nat Neurosci 7:764–772.

Krekelberg B, van Wezel RJ, Albright TD (2006) Adaptation in macaque MT reduces perceived speed and improves speed discrimination. J Neurophysiol 95:255–270.

Leopold DA, O'Toole AJ, Vetter T, Blanz V (2001) Prototype-referenced shape encoding revealed by high-level aftereffects. Nat Neurosci 4:89–94.

Lisberger SG, Movshon JA (1999) Visual motion analysis for pursuit eye movements in area MT of macaque monkeys. J Neurosci 19:2224–2246.

Maffei L, Fiorentini A, Bisti S (1973) Neural correlate of perceptual adaptation to gratings. Science 182:1036–1038.

Matsui T, Koyano KW, Koyama M, Nakahara K, Takeda M, Ohashi Y, Naya Y, Miyashita Y (2007) MRI-based localization of electrophysiological recording sites within the cerebral cortex at single-voxel accuracy. Nat Methods 4:161–168.

Merigan WH (2000) Cortical area V4 is critical for certain texture discriminations, but this effect is not dependent on attention. Vis Neurosci 17:949–958.

Merigan WH, Pham HA (1998) V4 lesions in macaques affect both single- and multiple-viewpoint shape discriminations. Vis Neurosci 15:359–367.

Miller EK, Gochin PM, Gross CG (1991) Habituation-like decrease in the responses of neurons in inferior temporal cortex of the macaque. Vis Neurosci 7:357–362.

Ohzawa I, Sclar G, Freeman RD (1985) Contrast gain control in the cat's visual system. J Neurophysiol 54:651–667.

Pasupathy A, Connor CE (1999) Responses to contour features in macaque area V4. J Neurophysiol 82:2490–2502.

Pasupathy A, Connor CE (2001) Shape representation in area V4: position-specific tuning for boundary conformation. J Neurophysiol 86:2505–2519.

Pasupathy A, Connor CE (2002) Population coding of shape in area V4. Nat Neurosci 5:1332–1338.

Paxinos G, Huang X-F, Toga AW (2000) The rhesus monkey brain. London: Academic Press.

Perlman I, Normann RA (1998) Light adaptation and sensitivity controlling mechanisms in vertebrate photoreceptors. Prog Retin Eye Res 17:523–563.

Reynolds JH, Chelazzi L, Desimone R (1999) Competitive mechanisms subserve attention in macaque areas V2 and V4. J Neurosci 19:1736–1753.

Saleem KS, Logothetis NK (2007) A combined MRI and histology atlas of the rhesus monkey brain in stereotaxic coordinates. London: Academic Press, Elsevier Limited.

Sanchez-Vives MV, Nowak LG, McCormick DA (2000) Membrane mechanisms underlying contrast adaptation in cat area 17 in vivo. J Neurosci 20:4267–4285.

Sawamura H, Orban GA, Vogels R (2006) Selectivity of neuronal adaptation does not match response selectivity: a single-cell study of the FMRI adaptation paradigm. Neuron 49:307–318.

Smirnakis SM, Berry MJ, Warland DK, Bialek W, Meister M (1997) Adaptation of retinal processing to image contrast and spatial scale. Nature 386:69–73.

Sobotka S, Ringo JL (1994) Stimulus specific adaptation in excited but not in inhibited cells in inferotemporal cortex of macaque. Brain Res 646:95–99.

Suzuki S (2001) Attention-dependent brief adaptation to contour orientation: a high-level aftereffect for convexity? Vis Res 41:3883–3902.

Suzuki S (2003) Attentional selection of overlapped shapes: a study using brief shape aftereffects. Vis Res 43:549–561.

Suzuki S, Cavanagh P (1998) A shape-contrast effect for briefly presented stimuli. J Exp Psychol Hum Percept Perform 24:1315–1341.

Webster MA, MacLin OH (1999) Figural aftereffects in the perception of fæces. Psychon Bull Rev 6:647–653.

Webster MA, Mollon JD (1991) Changes in colour appearance following post-receptoral adaptation. Nature 349:235–238.

APPENDIX

Supplementary data

Supplementary data associated with this article can be found, in the online version, at doi:10.1016/j.neuroscience.2009.03.070.

(Accepted 30 March 2009)
(Available online 5 April 2009)